FORSCHUNGSZENTRUM
ROSSENDORF e.V.

FZR

FZR-41
May 1994
Preprint

B. Heide and H.W. Barz

Effects of Flow on Intermediate Mass Fragments in Central Gold on Gold Collisions

Effects of Flow on Intermediate Mass Fragments in Central Gold on Gold Collisions

B. Heide[a,b] and H.W. Barz [b,a]

[a] Institut für Kern- und Hadronenphysik, FZ Rossendorf,
Pf 510119, D-01314 Dresden, Germany
[b]Institut für Theoretische Physik, Technische Universität Dresden,
Mommsen Str. 13, D-01062 Dresden, Germany

Abstract

Nearly central *Au* on *Au* collisions at 150 MeV/u are investigated. The properties of the fragmenting source are determined by the Boltzmann-Ühling-Uhlenbeck approach. A statistical multifragmentation model including secondary decay and Coulomb expansion is used to describe the final decay. A reduced anisotropic radial flow is needed to reproduce the relative velocity distributions.

1. Introduction

With the present day accelerators heavy ion collisions can be studied in a wide range of bombarding energies beginning from the onset of the multifragmentation up to a regime of total break-up into single nucleons. The fall and rise [1] of multifragmentation was observed in peripheral *Au* on *Au* collisions as a function of the excitation energy of the system. Theoretical studies [2, 3] of the data based on the statistical multifragmentation models show that a maximum number of intermediate mass fragments (IMFs) are formed at excitation energies between 5 and 10 MeV per nucleon depending on the mass number of the system. The basic assumption of the statistical models [4, 5, 6] is that the energy is equally distributed among the available degrees of freedom. However, even in central collisions at bombarding energies of several hundreds of MeV a surprisingly large number of IMFs is produced [7, 8]. This shows that not all the energy can be distributed randomly. The leak-out of pre-equilibrium particles and the appearance of ordered collective motion of the nuclear matter could explain that only a limited amount of energy is distributed statistically.

The occurrence of collective nuclear motion is essential for the hydrodynamical

treatment of nuclear collisions [9]. The flow is observed in experiment most easily by measuring the kinetic energy of the fragments as a function of their mass. The characteristic increase was observed in the sideflow and the squeeze-out [10]. Recently, large radial flow was seen in central collisions of sufficiently large projectiles and target nuclei [11, 12, 13, 14, 15] whereas in peripheral collisions no radial flow was found [11, 16].

Microscopically the motion of nucleons is fairly well understood within transport models. However the description of the formation of fragments is still an open problem. A quantum mechanical treatment by coupled transport equations [17] allows one to describe only light cluster formation, while the quantum molecular dynamic approach suffers from the inability to describe the final state of the fragments by quantum effects [18]. So it is an open question how the collective motion of the nucleons is transferred to the fragments.

It is our aim to analyse recent data of central Au in Au collisions at 150 MeV beam energy (see ref. [7, 14, 15, 19]) and to study to what an extent flow is present in the measured IMFs. Therefore, we simulate central collisions within the frame of the Boltzmann-Ühling-Uhlenbeck (BUU) approach. From this calculation we extract in section 2 the properties of the fragmenting source including the collective nucleonic motion. These results will be incorporated in the statistical multifragmentation model placing the fragments in accordance with the space-momentum distribution of the nucleonic matter calculated in the BUU model. Then, we let the system evolve under the influence of the mutual Coulomb repulsion while the excited fragments still cool down by emission of light particles.

To compare our results to the data we calculate in section 3 the kinetic energy spectra of the fragments and the two-particle velocity distribution $Y_{12}(v_{12})$ depending on the relative velocity v_{12}. Further, we investigate the correlations of the fragments via the two-particle correlation-function:

$$C_2(v_{12}) = \frac{Y_{12}(v_{12})}{Y_{12,mix}(v_{12})}, \tag{1}$$

where $Y_{12,mix}(v_{12})$ denotes the two-particle velocity distribution calculated by mixing two different events. Both distributions are normalized according to $\int dv_{12} Y_{12} = 1$. The correlation C_2 is widely used (see e.g. [20]) to provide information on the break-up size and the time duration of the fragmentation process. It will be shown that the correlation C_2 is also sensitive to the collective nucleonic flow.

2. Analysis of BUU calculations

To gain insight in the reaction mechanism we apply the BUU approach for the collision of Au on Au at 150 MeV per nucleon. The BUU approach, described in

detail in ref. [21], generates the phase space distribution $f(\mathrm{r},\mathrm{p},t)$ by averaging over parallel ensembles of pseudo-nucleons. This BUU calculation is expected to give a good estimate of the degree of thermalization in the violent stage of the collision. The nucleons are assumed to move in a collectively generated mean field and interact pairwise with each other through two-body collisions obeying the Pauli exclusion principle.

We use this approach to calculate the density profile as well as energy and momentum distributions of the matter in different regions of the coordinate space at a certain break-up time after which we assume that the fragmentation process sets in. Following the time evolution we recognize that a considerable number of fast particles leave the collision zone early and move within highly diluted matter. These pre-equilibrium particles are too far away from each other to participate in the fragmentation process. To exclude these particles we introduce a limiting density n_{limit}. We consider only those parts of matter, the density of which is larger than n_{limit} at break-up time. The pre-equilibrium particles take away a large part of the energy of the system. Therefore, the excitation energy of the remaining matter becomes moderate and is much smaller than one expects if the bombarding energy is equally shared among all nucleons.

Neither in coordinate nor in momentum space the distributions are spherical. Their shape changes strongly with impact parameter. To account for this fact we choose a coordinate system given by the energy flow tensor

$$\Theta_{ij} = \frac{1}{N}\sum_n \frac{p_i^{(n)} p_j^{(n)}}{2m_N}, \tag{2}$$

where the sum runs over all N nucleons with $p_i^{(n)}$ being the i-th component of the nucleon momentum $p^{(n)}$ in the centre-of mass frame of the considered piece of matter, and m_N denotes the nucleon mass. Thermal as well as collective motion contribute to the energy flow tensor. The new frame is defined by the three eigenvectors $e^{(i)}(i = 1,2,3)$ of the energy flow tensor Θ. The 3-axis of the internal system is identified by that eigenvector $e^{(3)}$ which deviates by the smallest angle from the beam axis.

To determine the energy which is contained in the flow we calculate the three flow components F_i

$$F_i = \frac{1}{2m_N} \frac{\left[\frac{1}{A}\sum_n (p^{(n)}\cdot e^{(i)})(r^{(n)}\cdot e^{(i)})\right]^2}{\frac{1}{A}\sum_n (r^{(n)}\cdot e^{(i)})^2}. \tag{3}$$

These definitions generalize the radial flow [12], $F_{radial} = \left[\sum_n p^{(n)}\cdot r^{(n)}\right]^2 / \left[2m_N A \sum_n (r^{(n)})^2\right]$, which is a convenient measure in nearly spherically expanding systems. In general the unequality relations $\sum \Theta_{ii} \geq \sum F_i \geq F_{radial}$ hold.

From the BUU calculations we extract further the excitation energy per particle E^* as sum of the potential energy, the Coulomb energy and the kinetic energy

relative to the binding energy of normal nuclear matter E_0:

$$E^* = E_{pot}/A + E_{coul}/A + \frac{m_N}{2}\langle v_{loc}^2\rangle - E_0. \qquad (4)$$

The kinetic energy is calculated with the velocity v_{loc} of the pseudo particle relative to the velocity of the cell calculated as the ensemble average over all pseudo particles.

We have compared different equations of states within the BUU approach, namely $E_{pot}/A = -c_1\,(n/n_0) + c_2\,(n/n_0)^\sigma$ as a function of the particle density n relative to the normal nuclear matter density n_0. We use $c_1 = 178$ MeV, 109 MeV, 62 MeV; $c_2 = 139.8$ MeV, 70.3 MeV, 23.5 MeV; $\sigma = \frac{7}{6}, \frac{4}{3}, 2$ for the soft , the medium and the hard equation of state, respectively.

In fig. 1 we have represented the excitation energy, the mass number, the transverse and the longitudinal flow energy as a function of the impact parameter for two different limiting densities $n_{limit} = 0.08n_0$ and $0.15n_0$ at a time of 70 fm/c after the moment of touching of the two nuclei. One recognizes that the region with $n < n_{limit}$ is only moderately excited. For a larger value of n_{limit} the size and the excitation energy of the central zone decrease. The smaller the impact parameter the higher the excitation energy is. Further, the flow pattern for impact parameters smaller than 1.5 fm has an oblate shape. For larger impact parameters the system becomes prolate, and its one-source character changes eventually into a two-source one. In the limit of large impact parameters the longitudinal flow F_3 approaches the energy of the relative motion while the transverse flow energy vanishes. The results of fig. 1 have been calculated by use of the medium equation of state. If we choose different equations of state the excitation energy is the only quantity which is remarkably affected. The value of the excitation energy is increased (reduced) by 0.7 MeV for the hard (soft) equation of state in comparison with the values in fig. 1. The flow values are nearly independent of the limiting density.

For the break-up time chosen the average density lies between $n_0/4$ and $n_0/3$. At such densities the matter has already reached the instability region and one expects that multifragmentation sets in provided the system has sufficient time to create fragments from the growing instabilities. In ref. [2] the break-up time was determined to be 90 fm/c by comparing the number of produced IMFs as a function of the number of all charges bound in fragments. However in more central collisions the density decreases faster. Therefore we use in our calculations a smaller break-up time of 70 fm/c and a limiting density of $n_{limit} = 0.15n_0$. A similar value of $n_{limit} = n_0/8$ was used in ref. [12] to describe reactions at lower energy.

3. Energy spectra and correlation function

In the experiment [7, 14] we are analysing multiplicity cuts were used to select central collisions with impact parameters b smaller than 4 fm. We report on

calculations with impact parameters between 0 and 3 fm in steps of 1 fm.

Now we employ the Copenhagen statistical multifragmentation model [5]. This model starts with the situation at break-up time. An ensemble of systems containing hot fragments is generated using the mass number, the excitation energy and the break-up volume corresponding to fig. 1. A system decays into 32 hot fragments in the average. There are approximately 17 IMFs with charges larger than two among these fragments. The crack width, i.e. the average distance between two fragments, amounts to 3.6 fm which is compatible with the standard value of 2.8 fm. The break-up volume has an ellipsoidal shape. Its deformation is taken from the BUU calculation. It turned out that the shape does not influence sensitively the final velocity distribution of the fragments.

Next, we incorporate the flow by giving the fragments an initial velocity. Each velocity component v_i is taken to be proportional to the distance from the centre and the amount is chosen such that the flow energies F_i are obtained. Further, a random thermal velocity given by the kinetic temperature is superimposed. We used a kinetic temperature of 15 MeV compatible with the kinetic enenrgy distribution found in the BUU calculations. This kinetic temperature could survive the fragment formation as it was demonstrated in ref. [22].

The time evolution of these hot sources is calculated under the influence of the Coulomb force. During the expansion the fragments evaporate light and heavier particles with excitation energies up to 8 MeV. The evaporation times are calculated by using the Weisskopf model (see ref. [5]). As a result of the expansion the final multiplicity is increased to about 100 particles while the number of IMFs is reduced to about seven. Finally the events are boosted with the centre-of-mass velocity and the reaction plane is rotated by a random azimuthal angle.

Using the experimental cuts of the 4π-detector [8] a representative ensemble of events is selected. In fig. 2a we represent the distribution Y_{12} and in fig. 2c the correlation function C_2 of eq. (1). To combine the data for different IMFs the distributions are shown as a function of the reduced velocity $v_{red} = v_{12}/\sqrt{Z_1 + Z_2}$ which is advantageously used when discussing the suppression at small relative velocities [23]. It is obvious that the velocity distribution of the IMFs peaks at too a large velocity value. This large relative velocity is caused by the flow. This means that the flow extracted from the BUU calculations is too large for the IMFs. The results shown in fig. 2b and fig. 2d are obtained by reducing the flow in transverse direction by 50 %. This reduction leads to a fair agreement of the distribution function as well as the correlation function C_2 with the data. It suggests that heavier fragments are formed in more central regions.

Comparing the two figures one recognizes that the two-particle correlation function is sensitive to the flow values at small relative velocities. The radial motion of the IMFs increases the width of the Coulomb hole while thermal motion and fragment evaporation act oppositely. Therefore, these effects have to be considered appropriately in order to extract source radii from the IMF analysis. Our results are compatible with a source radius of 11 fm consisting of 220 nu-

cleons. The occurrence of the flat maximum at $v_{red} = 0.04c$ is connected with the sideways flow of the matter. Already for an impact parameter of 3 fm the flow ellipsoid is strongly stretched in the direction of the flow angle of 35 degrees which gives a wider velocity distribution for $Y_{12mix}(v_{red})$ than for $Y_{12}(v_{red})$.

The one-particle variables are also fairly well reproduced using the reduced flow. In fig. 3 we compare the double differential cross section as a function of the kinetic energy in the centre-of-mass system with experiment [19]. The reduced flow is sufficient to explain the flat energy spectra for Li, Be, B and C isotopes. One can extract the flow energy by fitting the mean kinetic energies from these data. This procedure gives a flow value of 19 MeV per nucleon which is in rough agreement with experiment [14]. This value is affected by a energy gain during the final expansion while the average radial flow at break-up, taken as input, was 12 MeV. This value is significantly determined by the longitudinal component F_3 for the impact parameter b=3 fm. No agreement is reached for hydrogen isotopes. In our calculation (solid line) most of them are evaporated from hot fragments. The dashed line represents the spectrum of the pre-equilibrium protons which is also too steep. However, it is known that the pre-equilibrium protons coalesce with neutrons to deuterons and tritons. This mechanism gives the hydrogen isotopes a larger kinetic energy and produces a flatter spectrum. Our model cannot account for this effect. Similarly, the deviation seen in the He spectrum may be caused by coalescence too.

4. Conclusions

Our aim was to understand the velocity distributions of IMFs measured in central Au on Au collisions starting from the nucleonic velocity field calculated in the BUU approach. To calculate the number of IMFs we applied a statistical model. We found that a central region consisting of roughly half of the total number of nucleons has a sufficient small excitation energy of about 10 MeV. The fragmentation of this region can account for the measured charge distribution. As an important free parameter a limiting density n_{limit} is used below which multifragmentation is ruled out. This criteria defines a single source for small impact parameters. For larger impact parameters a two source model is more appropriate.

The BUU calculations predict an oblate nucleonic flow of 12 MeV in very central collisions with impact parameters around 1 fm. This value does not contain the final Coulomb push after break-up. Already at impact parameters around 3 fm the flow becomes very asymmetric and is dominant in forward direction. We found that only a part of the flow energy is transferred to the IMFs. To fit the experiment a reduction of the transverse flow energy by a factor of two is used. The same degree of agreement could also be reached by reducing the flow in all directions to 2/3 of its value. We have preferred the first version keeping in mind that the longitudinal flow has to converge to the kinetic energy of the rel-

ative motion in the limit of large impact parameters. The average radial flow at break-up found in our analysis is about 12 MeV. This result relies essentially on our assumption on the impact parameter selection. A careful inspection of fig. 3 indicates also that for light isotopes like Li the flow is not so strongly reduced as for the heavier isotopes. Such tendency was also reported in ref. [16].

The radial flow effects strongly the correlation function C_2 increasing the range of relative velocities where Coulomb suppression occurs. The agreement with experiment could be improved by using a kinetic temperature of 35 MeV as proposed recently [24]. Such a high temperature cannot be present in the initial stage but could be generated during the fragmentation process due to the release of the binding energy of the IMFs. Our evaporation model seems not to lead to such a large increase of the final temperature of the IMFs.

We thank B. Kämpfer, R. Kotte, W. Neubert, D. Wohlfahrt, W. Reisdorf, W. Trautmann and P. Danielewicz for stimulating discussions. H.W. B. and B. H. acknowledge support by the German BMFT under contract 06DR107.

References

[1] C.A. Ogilvie *et al.* , Phys. Rev. Lett. 67 (1991) 1214.

[2] H.W. Barz, W. Bauer, J.P. Bondorf, A.S. Botvina, R. Donangelo, H. Schulz and K. Sneppen, Nucl. Phys. A561 (1993) 466.

[3] Bao-An Li, A.R. DeAngelis D.H.E. Gross, Phys. Lett. B303 (1993) 225.

[4] S.E. Koonin and J. Randrup, Nucl. Phys. A356 (1981) 223; Nucl. Phys. A474 (1987) 173.

[5] J.P. Bondorf, R. Donangelo, I.N. Mishustin, C. J. Pethick, H. Schulz and K. Sneppen, Nucl. Phys. A443 (1985) 321; J.P. Bondorf, R. Donangelo, I.N. Mishustin and H. Schulz, Nucl. Phys. A444 (1985) 460; H.W. Barz, J.P. Bondorf, R. Donangelo, I.N. Mishustin and H. Schulz, Nucl. Phys. A448 (1986) 753.

[6] Sa Ban-hao and D.H.E. Gross, Nucl. Phys. A437 (1985) 643;
X.Z. Zhang, D.H.E. Gross and Y.M. Zheng, Nucl. Phys. A461 (1987) 641; Nucl. Phys. A461 (1987) 668.

[7] J.P. Alard et al., Phys. Rev. Lett. 69 (1992) 889.

[8] P. Kreutz *et al.* , GSI Preprint 92-23 (1992).

[9] W. Scheid. B. Müller and W. Greiner, Phys. Rev. Lett. 32 (1974) 741;
M. Sobel, P. Siemens, J. Bondorf and H. Bethe, Nucl. Phys. A251 (1975) 302.

[10] H. Stöcker and W. Greiner, Phys. Rep. 137 (1986) 277.

[11] H.W. Barz, J.P. Bondorf, R. Donangelo, R. Elmér, F.S. Hansen, B. Jakobsson, L. Karlsson, H. Niefenecker, H. Schulz, F. Schüssler, K. Sneppen and K. Söderström, Nucl. Phys. A531 (1991) 453.

[12] D.R. Bowman *et al.* Phys. Rev. C46 (1992) 1834.

[13] W. Bauer, J.P. Bondorf, R. Donangelo, R. Elmér, B. Jakobsson, H. Schulz, F. Schüssler, and K. Sneppen, Phys. Rev. C47 (1993) R1838.

[14] N. Hermann, Proc. Int. Nuclear Physics Conf. July 26 - Aug. 1, 1992, Wiesbaden, Germany, Nucl. Phys. A553 (1993) 739c.

[15] B. Kämpfer, R. Kotte, J. Mössner, W. Neubert, D. Wohlfahrt and FOPI collaboration, Phys. Rev. C48 (1993) R955.

[16] W. Trautmann, Proc. Int. Workshop XXII on Gross Properties of Nuclei and Nuclear Excitations, Edt. H. Feldmeier, W. Nörenberg, Hirschegg, Austria, Jan. 17-22, 1994, p. 10.

[17] P. Danielewicz and G.F. Bertsch, Nucl. Phys. A533 (1991) 712;
P. Danielewicz and Q. Pan, Phys. Rev. C47 (1992) 2002.

[18] J. Aichelin, Phys. Rep. 202 (1991) 233.

[19] S.C. Jeong et al. (FOPI), GSI preprint GSI-93-38 (1993).

[20] S.E. Koonin, Phys. Lett. B70 (1977) 43; S. Pratt and M.B. Tsang, Phys. Rev. C36 (1987) 2390.

[21] W. Bauer et al., Phys. Rev. C 34 (1986) 2127;
W. Bauer, Phys. Rev. Lett. 61 (1988) 2534.

[22] H.W. Barz, H. Schulz and G.F. Bertsch, Phys. Lett. B 217 (1989) 397.

[23] Y.D. Kim, R.T. de Souza, C.K. Gelbke, W. Gong and S. Pratt, Phys. Rev. C45(1992)387.

[24] B. Kämpfer, R. Kotte, J. Mössner, W. Neubert and D. Wohlfahrt, Proc. Int. Workshop XXII on Gross Properties of Nuclei and Nuclear Excitations, Edt. H. Feldmeier, W. Nörenberg, Hirschegg, Austria, Jan. 17-22, 1994, p. 113.

Figure caption

Fig. 1. Calculated excitation energy E^*, mass number A, transverse flow $(F_1 + F_2)/2$ and longitudinal flow F_3 as a function of the impact parameter for two limiting densities of 0.08 n_0 (circles), and 0.15 n_0 (stars), respectively.

Fig. 2. Velocity distribution Y_{12} and correlation function C_2 as a function of the reduced velocity for central Au on Au collisions compared to the experiment [15]. The calculated curves in panels (a) and (c) refer to full flow, whereas those in panels (b) and (d) correspond to a reduced flow.

Fig. 3. Calculated energy spectra in the centre-of-mass system (small dots connected by line) compared to data [19] (big dots) for light elements. The data are normalized by a common factor to fit the Li isotpes. The dashed line in the first frame shows the spectrum of pre-equilibrium protons.

Fig. 1

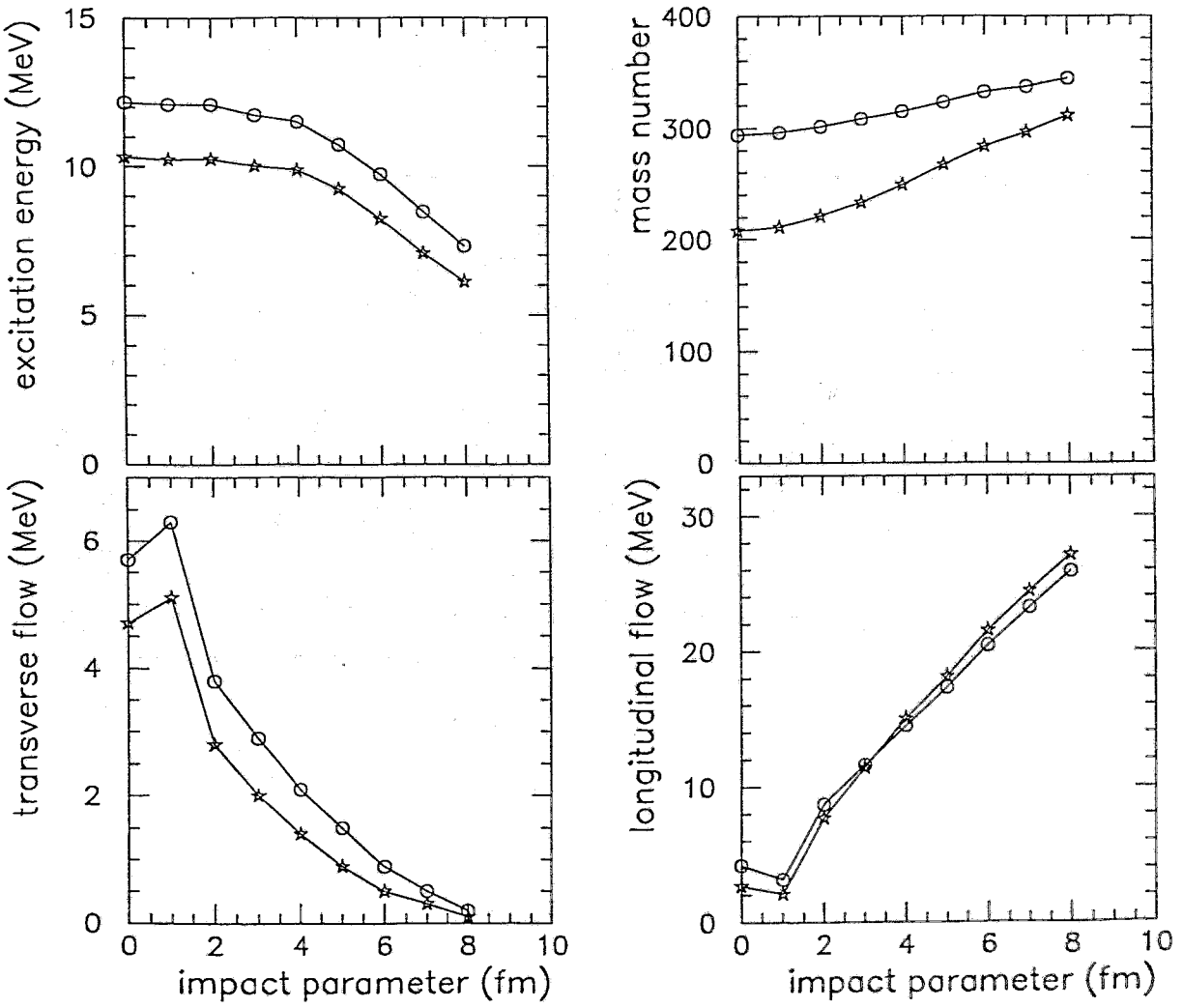
excitation energy (MeV)
15
10
5
0
transverse flow (MeV)
6
4
2
0
0
2
4
6
8
10
impact parameter (fm)
mass number
400
300
200
100
0
longitudinal flow (MeV)
30
20
10
0
0
2
4
6
8
10
impact parameter (fm)

Fig. 2

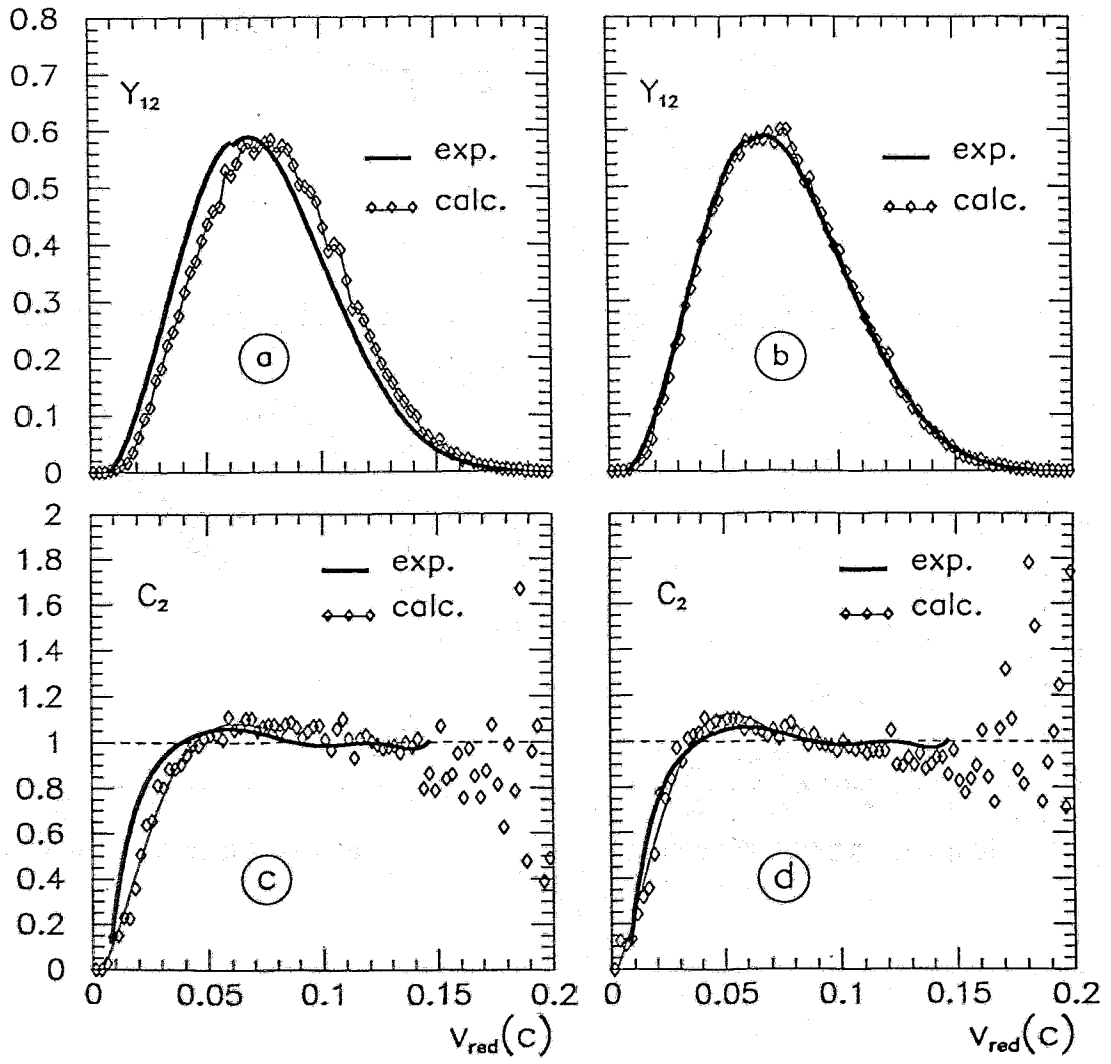
0.8
0.7
0.6
0.5
0.4
0.3
0.2
0.1
0
Y_{12}
exp.
calc.
a
b
2
1.8
1.6
1.4
1.2
1
0.8
0.6
0.4
0.2
0
C_2
c
d
0
0.05
0.1
0.15
0.2
$V_{red}(c)$

Fig. 3

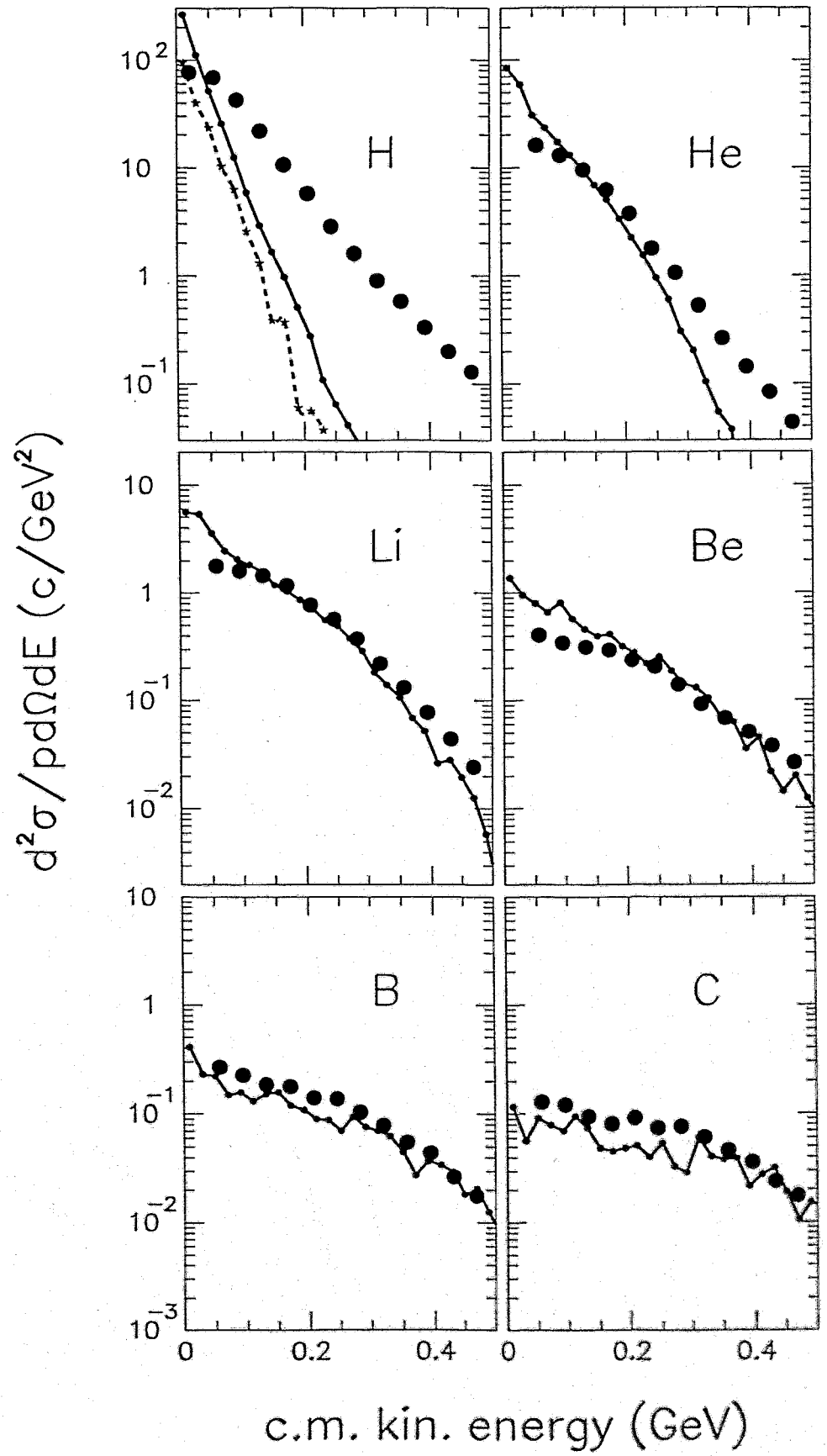
H
He
Li
Be
B
C
10^2
10
1
10^{-1}
10^{-2}
10^{-3}
0
0.2
0.4
$d^2\sigma/pd\Omega dE$ (c/GeV^2)
c.m. kin. energy (GeV)